NANO LETTERS

Letter

pubs.acs.org/NanoLett

Novel Two-Dimensional Silicon Dioxide with in-Plane Negative Poisson's Ratio

Zhibin Gao,[†,§,⊥] Xiao Dong,[*,‡] Nianbei Li,[†,§,⊥] and Jie Ren[*,†,§,⊥]

[†]Center for Phononics and Thermal Energy Science, School of Physics Science and Engineering, Tongji University, 200092 Shanghai, P. R. China

[‡]Center for High Pressure Science and Technology Advanced Research, Beijing 100193, China

[§]China-EU Joint Center for Nanophononics, School of Physics Science and Engineering, Tongji University, 200092 Shanghai, P. R. China

[⊥]Shanghai Key Laboratory of Special Artificial Microstructure Materials and Technology, School of Physics Science and Engineering, Tongji University, 200092 Shanghai, P. R. China

Supporting Information

ABSTRACT: Silicon dioxide or silica, normally existing in various bulk crystalline and amorphous forms, was recently found to possess a two-dimensional structure. In this work, we use ab initio calculation and evolutionary algorithm to unveil three new two-dimensional (2D) silica structures whose thermal, dynamical, and mechanical stabilities are compared with many typical bulk silica. In particular, we find that all three of these 2D silica structures have large in-plane negative Poisson's ratios with the largest one being double of penta graphene and three times of borophenes. The negative Poisson's ratio originates from the interplay of lattice symmetry and Si—O tetrahedron symmetry. Slab silica is also an insulating 2D material with the highest electronic band gap (>7 eV) among reported 2D structures. These exotic 2D silica with in-plane negative Poisson's ratios and widest band gaps are expected to have great potential applications in nanomechanics and nanoelectronics.

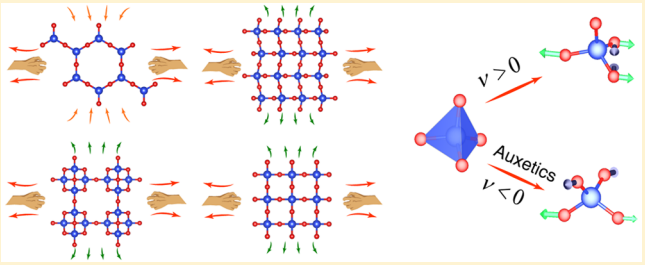

KEYWORDS: *Two-dimensional material, silicon dioxide, in-plane negative Poisson's ratio, 2D material with widest band gap, crystal structure searching*

Silicon dioxide with the chemical formula SiO_2 is the fundamental component of glass, sand, and most minerals and is also known as one of the building units of earth crust and mantle. There are a large number of isomers with the formula of SiO_2 in crystalline and amorphous forms, such as quartz, , and glassy SiO_2. In all of the known SiO_2 compounds, Si has sp^3 hybridization with 4-fold tetrahedron configuration. O is coordinated with 2 Si atoms but sometimes with angle type like O in H_2O and sometimes with linear type like C in CO_2. The variety of SiO_2 phases mainly originates from the space stacking form of Si−O tetrahedron. Normally, bulk silicon dioxides are hard (α-quartz with theoretical Vickers hardness 30.2 GPa[1]), high-quality electrical insulators and favorable dielectric materials. Because of the outstanding mechanic and electronic performances, SiO_2 films and slabs have significant applications in mechanics, optics, and electronics.

Two-dimensional (2D) materials are substances with a monolayer or few atomic layers thickness[2,3] (Figure 2). Because of quantum confinement effect, electrons in these materials only have freedom in 2D plane, which could give rise to new physics. But so far, the 2D materials are quite rare and most of them are semimetals (for example, graphene) or semiconductors (for example, black phosphorus, sulfide, and selenide) with few being insulators, for example, h-BN, the reported insulating 2D structure with the widest band gap (4.7 eV theoretically[4−6] and 6.4 eV experimentally[7]). It is well-known that 3D silicon dioxide is a good insulator with wide band gap. Therefore, it is interesting to explore whether the corresponding 2D counterpart may also be stable as a monolayer and exhibit novel properties. If confirmative, it is likely to make contributions to transistors of nanomaterials and multifunctional van der Waals (vdW) heterostructures.[8,9]

Thin silica film has first been grown on metal Mo(112) substrate.[10−13] Then slab crystalline silica sheet is grown on another metal Ru(0001).[14,15] Furthermore, this hexagonal quasi-2D silica can even be supported by graphene.[16] In this Letter, we focus on the intrinsic mechanical porperties and use theoretical structure prediction to explore 2D crystalline freestanding silicon dioxide. We identify three novel stable 2D silica phases, besides the reported 2D silica.[14] They all

Received: September 19, 2016
Revised: January 12, 2017
Published: January 13, 2017

DOI: 10.1021/acs.nanolett.6b03921
Nano Lett. 2017, 17, 772−777

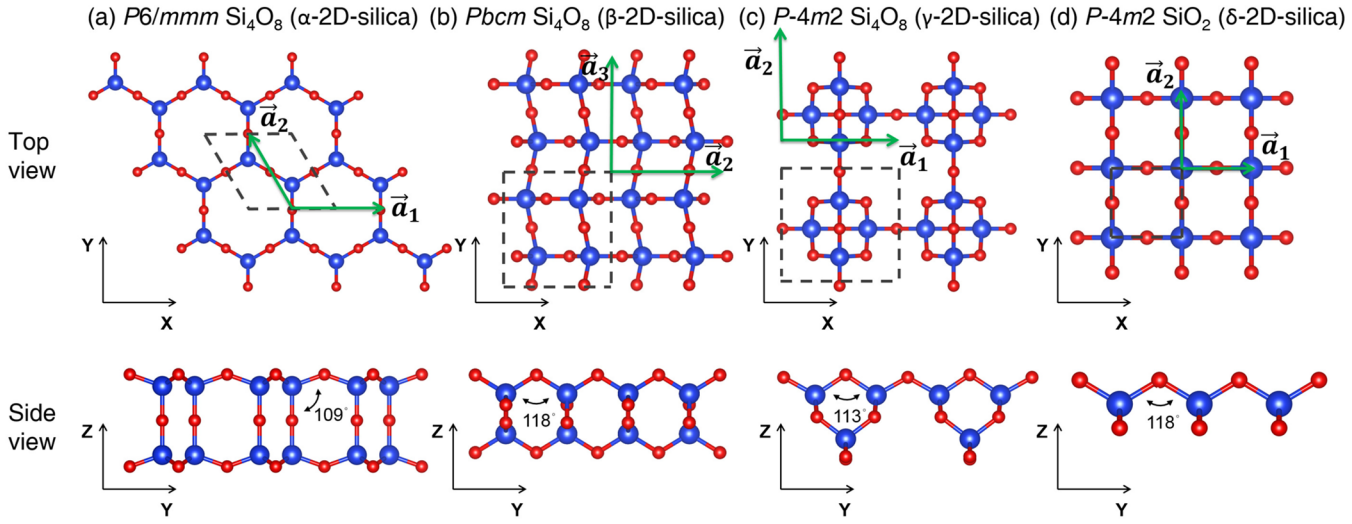

Figure 1. Equilibrium 2D monolayer silicon dioxide of (a) *P6/mmm* Si_4O_8 (α-2D silica), (b) *Pbcm* Si_4O_8 (β-2D silica), (c) *P-4m2* Si_4O_8 (γ-2D silica), and (d) *P-4m2* SiO_2 (δ-2D silica) in both top and side views. Large blue and small red balls in the (a–d) represent silicon and oxygen atoms, respectively. The Wigner–Seitz cells are shown by the dotted black regions. The green solid arrows show the lattice vectors.

Table 1. Optimized Structural Properties of the Four Different 2D Silicon Dioxide Crystal Structures[a]

phase	α-2D silica (Si_4O_8)	β-2D silica (Si_4O_8)	γ-2D silica (Si_4O_8)	δ-2D silica (SiO_2)
space group	*P6/mmm*	*Pbcm*	*P-4m2*	*P-4m2*
$\lvert\vec{a}_1\rvert$ (Å)	5.31	20.00	5.64	2.84
$\lvert\vec{a}_2\rvert$ (Å)	5.31	5.07	5.64	2.84
$\lvert\vec{a}_3\rvert$ (Å)	20.00	5.53	20.00	20.00
atomic positions	Si 4h (0.67,0.33,0.42)	Si 4d (0.55,0.70,0.25)	Si 4k (0.50,0.75,0.55)	Si 1d (0.00,0.00,0.50)
	O 6i (0.50,0.50,0.39)	O 4d (0.52,0.39,0.25)	O 2f (0.50,0.50,0.40)	O 2g (0.50,0.00,0.46)
	O 2d (0.33,0.67,0.50)	O 4c (0.59,0.75,0.50)	O 2g (0.50,0.00,0.59)	
			O 4i (0.73,0.27,0.50)	
E_c (eV/atom)	6.61	6.54	6.44	6.37
E_{G-HSE} (eV)	7.31	7.69	7.40	7.34
thickness (Å)	4.34	3.51	3.84	1.71

[a] $\lvert\vec{a}_1\rvert$, $\lvert\vec{a}_2\rvert$, and $\lvert\vec{a}_3\rvert$ are the lattice constants defined in Figure 1. Atomic positions are the group Wyckoff positions for each independent atoms in fractional coordinates. E_c is the cohesive energy per atom in eV. E_{G-HSE} is the band gap calculated by HSE06.

display in-plane negative Poisson's ratio (NPR), large band gaps, and superhard mechanical properties compared to 3D α-quartz.

Computational Details. Crystal structure searching was performed via the ab initio evolutionary algorithm in USPEX[17−19] that has been successfully applied to a wide range of searching problems.[20−22] Furthermore, we have reconfirmed the obtained four structures of global minimum free energy based on particle swarm optimization, implemented in CALYPSO code.[23] We sequentially used 1−6 times of chemical formula SiO_2 (up to 18 atoms) per unit cell for searches. According to the experimental results,[10,14] the thickness of hexagonal 2D silica is 4.34 Å. Therefore, in order to cover some extraordinary 2D silica, the original thickness was set up to 5 Å and permitted to relax during the evolution. The self-consistent energy calculations and structure optimization were employed using the Perdew–Burke–Ernzerhof (PBE) exchange-correlation functional[24] along with the projector-augmented wave (PAW) potentials[25,26] as implemented in the Vienna Ab initio Simulation Package (VASP).[27,28] The kinetic energy cutoff was 800 eV and tetrahedron method with Blöchl correction[29] was used to integrate the Brillouin-zone. Energy convergence value in self-consistent field (scf) loop was selected as 10^{-8} eV and a maximum Hellmann–Feynman forces is less than 0.1 meV/Å. Such a high criteria is found to be required to achieve convergence for phonon calculations and all the elastic-constant components. All the results in this paper is also checked with the local density approximation (LDA) functional.[30] Additionally, because both LDA and PBE approaches usually underestimate the band gap of semiconductor and insulator, we adopt the screened hybrid functional of Heyd, Scuseria, and Ernzerhof (HSE06)[31] for a more accurate calculation. Phonon dispersion curves were obtained using the Phonopy package.[32]

Results and Discussion. *Structures.* A number of low-energy structures had been searched and only the most stable four 2D structures obtained in our computations are discussed here, with space groups of *P6/mmm* Si_4O_8, *Pbcm* Si_4O_8, *P-4m2* Si_4O_8, and *P-4m2* SiO_2. For simplicity, we define them as α-, β-, γ-, and δ-2D silica, respectively. The optimized four silica structures were shown in Figure 1. α-2D silica is hexagonal and has been experimentally grown on Mo(112) and Ru(0001) surfaces,[10,14] whereas we obtain it intrinsically in a freestanding form. That the known structure has been rediscovered in our crystal structure prediction does validate the correctness of our computational method in high-throughout computing. The other three are our new discovered structures during the explorations. α-2D silica has a perfect sp^3 bonding network that

DOI: 10.1021/acs.nanolett.6b03921
Nano Lett. 2017, 17, 772−777

means all O atoms are connected to Si atoms with same solid angles 109°28′, that is, Si is in a perfect O tetrahedron. The lattice constant in our computation of α-2D silica is 5.31 Å which is in good agreement with the experimental data 5.2−5.5 Å.[10,14] This confirms the accuracy of our structure prediction and relaxation.

The optimized structural parameters of four structures are summarized in Table 1. In all of 2D silica, each silicon is connected with four oxygens, constituting a tetrahedron like bulk SiO_2. Therefore, silicon atoms share 4-fold coordinations and oxygen two, which means all atoms have no redundant valence electrons. In the top view, α-2D silica, like graphene, indeed has a hexagonal crystal structure, while the other three have rectangular crystal configurations. Specifically, β-2D silica is an anisotropic structure in orthorhombic lattice while γ-2D silica and δ-2D silica are isotropic in tetragonal lattice. In the side view, α-2D silica with mirror symmetry to $z = 0$ plane consists of a "double" layers Si_2O_3 substructures connected by intermediate Si—O—Si bonds oriented perpendicular to the surfaces. However, the other three structures have large inherent bucklings in their interlaminations and lost mirror symmetry relative to x−y plane at $z = 0$. α-2D silica and δ-2D silica each have only one uniform length of Si—O bond, wheras β-2D silica and γ-2D silica have three different bond lengths. In the top view, the Si—O bonds are like crossroads in β-2D silica, γ-2D silica, and δ-2D silica crystal structures.

The four phases of 2D silica have different arrangement of Si—O tetrahedrons. By geometry (directions of Si—O bonds consistent with lattice vectors, lattice types and whether have mirror symmetry relative to $z = 0$ plane), the above four structures can be divided into two classes, one is α-2D silica, the other are β-, γ-, and δ-2D silica. The latter class has special crossed orientation of chemical bonds which is seldom found in silicon dioxide crystalline forms.

A deeper insight is that Si—O tetrahedron of symmetry group T_d has two special orthogonal projections: one goes through a vertex and the center of its opposite face (3-fold axis); the other goes through on opposite edges (2-fold axis). For most bulk SiO_2 phases and α-2D silica, the lattice vector is along 3-fold axis, which means this direction is easy to build a spacial framework by Pauling's third rule[33] (rule of sharing of polyhedron corners, edges, and faces). The representative local structure is double tetrahedron structure of $[Si_2O_7]^{-6}$, which is the fundamental structure of α-2D silica and quartz. Here, when the structure is limited to two dimension, the expansion in three-dimensional space become not very important, and the lattice vector can build the slab along 2-fold axis to get β-, γ-, and δ-2D silica. These coupling of lattice symmetry and Si—O tetrahedron symmetry also are the origin of NPR which will be discussed later.

As quasi-2D structures, the atomic thickness of α-, β-, γ-, and δ-2D silica are 4.34, 3.51, 3.84, and 1.71 Å, respectively. If we add two van der Waals (vdW) radii of the outmost surface atoms,[34] their effective thicknesses are 7.38, 6.55, 6.88, and 4.75 Å, respectively. It is observed that δ-2D silica is the thinnest structure, while the thickness increases by the sequence of δ-, β-, γ-, and α-2D silica. β-, γ-, and δ-2D silica are thinner than α-2D silica, which implies they are more like pure two-dimensional structures and have more low dimensional effects. Lower thickness makes these three phases lose mirror symmetry and they do not have enough spaces for double tetrahedron structure of $[Si_2O_7]^{-6}$, which is why they have different Si—O bond orientations. In this way, β-, γ-, and δ-2D silica can be seen as a metastable intermediate products when the atoms build silica from zero thickness to α-2D silica.

Stability and Wide Bandgap. Now our first priority is to answer the question whether these new freestanding 2D silicon dioxide materials are stable. In normal condition, silica exists in many crystalline forms. Here we compare the free energies of our 2D silica structures and 3D counterparts in thermodynamics and the calculation are implemented in HSE06 method (Figure 2). Compared with α-quartz, which has the lowest

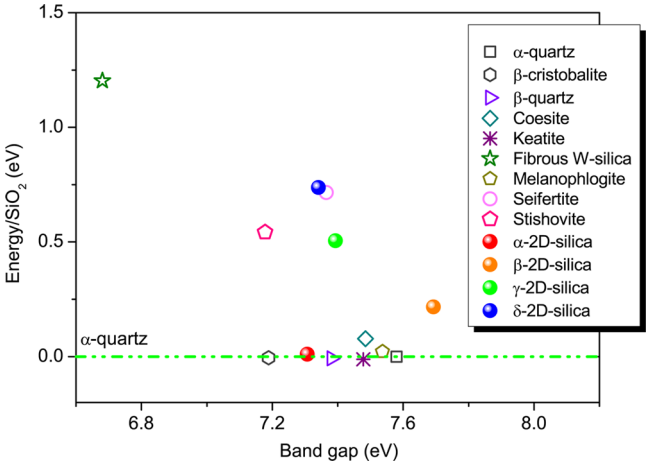

Figure 2. Energy landscape versus band gap of 3D and 2D silica materials as performed in the HSE06 method. As α-quartz is the most stable silica at low temperatures and is the most common form of crystalline silica, we set it as the benchmark reference in green dashed line to compare all silica structures.

energy to be the thermal-dynamically stable phase of SiO_2, all 2D silica are metastable phases. The structure of α-2D silica with highest symmetry has the lowest energy (0.047 eV/f.u.) in 2D silica and the energy is comparable to α-quartz that is chosen as the reference point of zero energy. Compared with other 2D silica, α-2D silica is thicker and more like bulk silica. That is why it has a similar energy to bulk quartz. Si—O bond length in α-2D silica is 1.63 Å with a quite similar to 1.61 Å of α-quartz, while the Si—O bonds are 1.64, 1.65, and 1.66 Å for β-, γ-, and δ-2D silica, respectively, which means there is a positive correlation between energy of structure and Si—O bond length since shorter distance intensifies the strength of Si—O bonds. In a word, $[SiO_4]$ tetrahedral unit in α-2D silica is more similar to α-quartz than β-, γ-, and δ-2D silica.

Besides, according to Pauling's fifth rule (parsimony rule[33]), the number of essentially different kinds of constituents in a crystal tends to be small. The repeating units will tend to be identical because each atom in the structure is most stable in a specific chemical environment. α-2D silica and α-quartz have only one type of tetrahedral, while β-, γ-, and δ-2D silica have two or three distorted tetrahedral because of symmetry breaking. Therefore, the energy of α-2D silica is close to bulk material with lower energy.

Though α-2D silica has been grown exprimentally,[10,13,14] it is not useless to explore other interesting phases with a little higher energy in complicated but brand new 2D silica energy landscape surface. As a matter of fact, metastable phases are ubiquitous in condensed matter, which do not produce a bad effect, but provide diverse structures transformation with vast applications to modern industrial societies and our daily life. The energies of β-2D silica (0.253 eV/f.u.), γ-2D silica (0.542

DOI: 10.1021/acs.nanolett.6b03921
Nano Lett. 2017, 17, 772−777

eV/f.u, and δ-2D silica (0.758 eV/f.u.) are comparable to stishovite[35,36] and seifertite[37] and are much lower than energy of fibrous W-silica.[38] Because stishovite and seifertite are observed by high-pressure experiments and quenchable to ambient condition, and W-silica can be synthesized by chemical methods, it is reasonable to believe that our three novel 2D phases can exist as metastable phases at normal conditions. It is also worth highlighting that β-2D silica has both the largest band gap (up to 7.69 eV) in our HSE06 calculations and a moderate low free energy.

The dynamical stability has been confirmed by calculating phonon dispersion relations shown in Figure S1. All the structures of four 2D silica are free from imaginary frequencies, which means they are dynamically stable. Furthermore, the dynamical stability of these freestanding 2D silica is also validated by performing ab initio molecular dynamics simulations using canonical ensemble at a series of elevated temperatures with lifetime longer than 10 ps (Figure S2). The result shows that all 2D silica are still robust even at high temperature (1000 K). Particularly, β-2D silica can live in the high temperature of 2500 K, which is much higher than the melting point of quartz (1986 K).[39]

For 2D elastic solid materials, mechanical stability is indispensable to the existence of materials. If a 2D material is mechanically stable, the corresponding elastic constants have to satisfy $C_{11}C_{22}-C_{12}^2 > 0$ and $C_{66} > 0$.[40] We have guaranteed that all the elastic constants (shown in Table S1) of four 2D silica always meet this compulsory requirement. Therefore, we have verified that α-, β-, γ-, and δ-2D silica are metastable phases.

Band gap is the fundamental electronic property for semiconductor and insulator. Theoretically, we find that 2D silica is of the largest band gap in all reported 2D crystal materials. As the electronic band structures are shown in Figure S3, α-, β-, γ-2D silica are direct insulators while δ-2D silica is an indirect insulator. Compared with h-BN which is reported to have a large band gap of 4.7 eV theoretically[4,6] (6.4 eV experimentally[7]), silica put the upper limit of 2D band gap to 7.69 eV. This implies it is hard to change its electronic states in 2D silica. Because the absorption of light is related to the band gap and the thickness, 2D silica can be the most transparent materials in the world.

As good insulators, 2D silica can be an outstanding candidate for dielectric materials. Dielectric constants of α-, β-, γ-2D silica, and δ-2D silica are 3.18, 2.42, 2.24 and 2.49, respectively. Notably, based on the formula of in-plane parallel capacitor $c = \varepsilon S/4\pi kd$, capacitance of δ-2D silica is around 1.76 times larger than α-quartz because it is 0.31 times thinner than α-quartz. This means it is a favorable dielectric material for next nanomaterials transistors such as 2D transistors and 2D electronic devices[41] and a supercapacitor candidate.[42]

Superhard Mechanical Properties with NPR. When a material is stretched in one direction, it usually contracts in the other two directions perpendicular to the applied stretching direction, the so-called positive Poisson's ratio (PPR). Most materials have a PPRs ranging from 0 to 0.5. From the classical theory of elasticity, for 3D isotropic materials, the Poisson's ratio cannot be less than −1.0 or greater than 0.5.[43] Materials with NPR have the property that when stretched, they become auxetic perpendicular to the applied force. These materials are also called auxetics by its auxetic property with external strain. This interesting phenomenon was first presented in foam structure in 1987.[44] Then materials with NPR attract a lot of scientific interest by their wide applications, such as single-layer graphene and graphene ribbons,[45,46] single-layer black phosphorus,[47−49] hα-silica,[50] penta graphene,[40] borophenes,[20] and semimetallic Be_5C_2,[51] and can be used in vanes for aircraft,[52] packing materials,[53] body armor, and national defense.[54] Furthermore, we find that in-plane NPR is rare and novel in 2D materials based on the collected data from the available published papers with our utmost endeavor shown in Figure S4.

Poission's ratio ν and Young's modulus E in the xy plane can be expressed as the following equations

$$\nu_{xy} = -\frac{d\varepsilon_y}{d\varepsilon_x}, \quad \nu_{yx} = -\frac{d\varepsilon_x}{d\varepsilon_y}$$
$$E_x = \frac{\sigma(\varepsilon_x)}{\varepsilon_x}, \quad E_y = \frac{\sigma(\varepsilon_y)}{\varepsilon_y} \tag{1}$$

where ν_{xy} is the Poisson's ratio of the x-direction that is induced by a strain in the x-axis. E_x is the Young's modulus of the x-direction that is the slope in the stress−strain curve. Similarly, ν_{yx} and E_y are the Poisson's ratio and Young's modulus in the y-direction. σ is the stress as a function of strain ε. We quantitatively calculated the Poisson's ratio ν and Young's modulus E for our four 2D silicon dioxides according to the eq 1 for uniaxial strain. The results of Poisson's ratio are shown in Figure 3. We also calculated the mechanical property by the elastic solid theory (the detailed description of this method is discussed in the Supporting Information). The results of elastic solid theory and strain method are quite similar (Table S2). Therefore, two methods confirm that our three 2D silica phases have NPR mechanical property. In order to check the correctness of our computational method and results, we select graphene and black phosphorus as references. Our results shown in Table S2 are in good agreement with the published results.[55−58] As we have mentioned above, α-2D silica, γ-2D silica, and δ-2D silica are isotropic materials, while β-2D silica is an anisotropic material. Therefore, except β-2D silica, all other three materials have the mechanical properties $E_x = E_y$ and $\nu_x = \nu_y$.

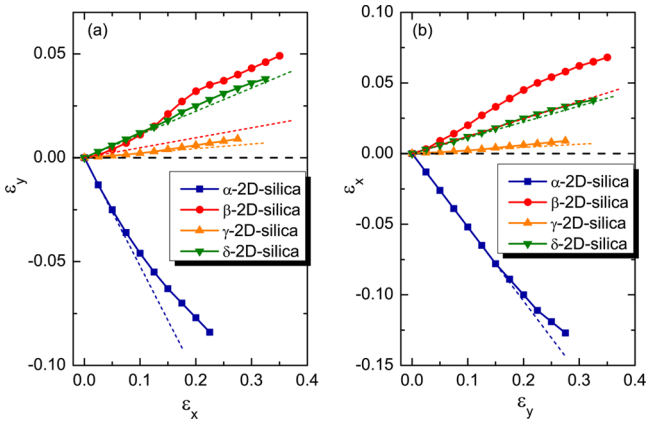

Figure 3. Poisson's ratio (short dashed lines denote the linear response counterpart) as a function of uniaxial tensile strain of α-2D silica, β-2D silica, γ-2D silica, and δ-2D silica in the (a) x-direction (ν_{xy} = 0.522, −0.048, −0.022, and −0.112) and (b) y-direction (ν_{yx} = 0.522, −0.123, −0.022, −0.112). The horizontal black dashed lines are set to zero for comparison.

DOI: 10.1021/acs.nanolett.6b03921
Nano Lett. 2017, 17, 772−777

Figure 3a displays the strain response in the y direction when applying stretch in the x-direction. Similarly, the Poisson's ratio of the y-direction is shown in Figure 3b. Obviously, there are two kinds of mechanical response when four 2D silica are stretched. α-2D silica is contracted perpendicular to the applied force, while β-2D silica, γ-2D silica, and δ-2D silica are auxetic during the uniaxial strain in 2D plane. Remarkably, β-2D silica in the y-direction and δ-2D silica in both x- and y-directions have large NPR values −0.123 and −0.112. These absolute values of NPR are quite high, that is, they are equal to double that of penta graphene (ν = −0.068),[40] three times that of borophenes (ν_x = −0.04, ν_y = −0.02),[20] and are different from single-layer black phosphorus whose NPR occurs in the yz plane.[47]

NPR of our novel three 2D silica structures originates from the low-dimensional effect. As discussed in Structures, [SiO_4] tetrahedron is the basic unit in both slab and bulk SiO_2. Normally, in a 3D system, by the request of sharing of polyhedron corners (Pauling's third rule[33]), the lattice is along the 3-fold axis of the Si—O tetrahedron. The tensile strain (in green arrows) on the direction of the median line of bottom of the tetrahedron makes the distance of two oxygen atoms decrease (in black arrows), which implies a positive Poisson's ratio (ν > 0) shown in Figure 4a. However, for 2D materials

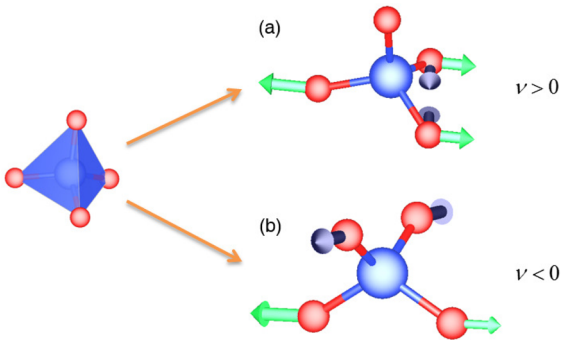

Figure 4. The explanation of Poisson's ratio for our new 2D silicon dioxide structures. Each silicon atom is surrounded by four oxygen atoms and due to its shape each SiO_4 group is called SiO_4 tetrahedron. (a) When the tensile strain (in green arrows) is applied to the direction of the median line of bottom of the tetrahedron (vertical to 3-fold axis) because of the angular variation, the distance of two oxygen atoms decreases (in black arrows), leading a positive Poisson's ratio (ν > 0). On the contrary, (b) when the tensile strain is applied to the edge to the tetrahedron (vertical to 2-fold axis), similarly because of the angular variation the distance of two oxygen atoms increases, leading a NPR phenomenon (ν < 0).

there is spatial constrains and the lattice can be along in the 2-fold axis. When the tensile strain is applied to the edge to the tetrahedron, the distance of two oxygen atoms increases, leading to the NPR phenomenon (ν < 0) shown in Figure 4b. Therefore, we believe the distinction between these two situations stems from the coupling of lattice symmetry and Si—O tetrahedron symmetry, which is a low-dimensional effect.

In a word, our three new structures are thinner than α-2D silica with stronger low-dimensional effect in geometry. This low-dimensional effect further leads to a different type of matching between lattice symmetry and Si—O tetrahedron symmetry, which finally leads to this interesting NPR phenomenon.[59]

We have also revealed the Young's modulus of these 2D silica materials and prove that they are superhard 2D materials. As we have explained above, we use the effective thickness of 2D materials, including two vdW radii.[34,60,61] The calculated Young's modulus are exhibited in Table S2. Generally, Young's modulus can be obtained by dividing the tensile stress by the extensional strain in the elastic region of the stress−strain graph. A material whose Young's modulus is high can be regarded as rigid. According to the experimental[62,63] and theoretical[64] values, the Young's modulus of 3D α-quartz is around 100 GPa at atmospheric pressure. It is to be disclosed that all four 2D silica are much harder than α-quartz. Young's modulus of δ-2D silica (346 GPa) is more than triple than that of α-quartz (100 GPa)[62−64] and is comparable to that of single-layer boron nitride (BN) (366 GPa).[65] Interestingly, the Young's modulus of β-2D silica in the y-direction (247 GPa) is more than double of that in the x-direction (97 GPa), which due to the strong anisotropy of its special crystal structures. The hardness of these 2D silica can be explained by tetrahedral silica structure in Figure 4 and phonon dispersion relations in Figure S1. The slope of phonon dispersions denotes the group velocity of each phonon. The bigger the group velocity, the more rigid the material is. Therefore, δ-2D silica and β-2D silica have a superhard and strong anisotropic mechanical properties.

Couclusion. In conclusion, we have performed a systematic structure searching and computationally guided material discovery for 2D silicon dioxide and found β-, γ-, and δ-2D silica. The thermal, dynamical, and mechanical stability checking guarantees that these 2D silica can exist as metastable phases at atmosphere condition. In particular, in-plane NPR has been identified in these three structures, whose values are so large that are double that of penta-graphene,[40] three times that of borophenes (ν_x = −0.04, ν_y = −0.02)[20] and are different from single-layer black phosphorus's NPR in the yz plane.[47] The NPR originates from the coupling of lattice symmetry and Si—O tetrahedron symmetry, which is a low dimensional effect. We have also proved these three 2D silica to be superhard materials, which indicate superior thermal conductivities compared to bulk silica materials. Furthermore, with its largest electronic band gaps in reported 2D crystal materials, we believe these novel 2D silica can be used as the most transparent insulators and good dielectric materials, which are expected to have great applications in many fields.

■ ASSOCIATED CONTENT

Supporting Information

The Supporting Information is available free of charge on the ACS Publications website at DOI: 10.1021/acs.nanolett.6b03921.

Additional figures, tables, methodology, and references (PDF)

■ AUTHOR INFORMATION

Corresponding Authors

*E-mail: xiao.dong@hpstar.ac.cn.
*E-mail: Xonics@tongji.edu.cn.

ORCID

Zhibin Gao: 0000-0002-6843-381X

Notes

The authors declare no competing financial interest.

DOI: 10.1021/acs.nanolett.6b03921
Nano Lett. 2017, 17, 772−777

■ ACKNOWLEDGMENTS

We thank our member Shenshen Yan for reconfirming the crystal structure searching results by CALYPSO. The numerical calculations were carried out at Shanghai Supercomputer Center. This work is supported by the National Youth 1000 Talents Program in China, and the 985 startup Grant (205020516074) at Tongji University (Z.G. and J.R.) and by the NSF China with Grant 11334007 (N.L.). X.D. also acknowledges the support of NSAF with Grant U1530402.

■ REFERENCES

(1) Chen, X.-Q.; Niu, H.; Li, D.; Li, Y. *Intermetallics* **2011**, *19*, 1275−1281.
(2) Geim, A. K.; Grigorieva, I. V. *Nature* **2013**, *499*, 419−425.
(3) Miro, P.; Audiffred, M.; Heine, T. *Chem. Soc. Rev.* **2014**, *43*, 6537−6554.
(4) Peng, Q.; De, S. *Phys. E* **2012**, *44*, 1662−1666.
(5) Churchill, H. O.; Jarillo-Herrero, P. *Nat. Nanotechnol.* **2014**, *9* (5), 330−331.
(6) Xu, Y.-N.; Ching, W. Y. *Phys. Rev. B: Condens. Matter Mater. Phys.* **1991**, *44*, 7787−7798.
(7) Zunger, A.; Katzir, A.; Halperin, A. *Phys. Rev. B* **1976**, *13*, 5560−5573.
(8) Liu, Y.; Weiss, N. O.; Duan, X.; Cheng, H.-C.; Huang, Y.; Duan, X. *Nat. Rev. Mater.* **2016**, *1*, 16042.
(9) Novoselov, K. S.; Mishchenko, A.; Carvalho, A.; Castro Neto, A. H. *Science* **2016**, *353*, 9439.
(10) Weissenrieder, J.; Kaya, S.; Lu, J.-L.; Gao, H.-J.; Shaikhutdinov, S.; Freund, H.-J.; Sierka, M.; Todorova, T. K.; Sauer, J. *Phys. Rev. Lett.* **2005**, *95*, 076103.
(11) Todorova, T. K.; Sierka, M.; Sauer, J.; Kaya, S.; Weissenrieder, J.; Lu, J.-L.; Gao, H.-J.; Shaikhutdinov, S.; Freund, H.-J. *Phys. Rev. B: Condens. Matter Mater. Phys.* **2006**, *73*, 165414.
(12) Schroeder, T.; Adelt, M.; Richter, B.; Naschitzki, M.; Bäumer, M.; Freund, H.-J. *Surf. Rev. Lett.* **2000**, *7*, 7−14.
(13) Seifert, J.; Blauth, D.; Winter, H. *Phys. Rev. Lett.* **2009**, *103*, 017601.
(14) Löffler, D.; Uhlrich, J. J.; Baron, M.; Yang, B.; Yu, X.; Lichtenstein, L.; Heinke, L.; Büchner, C.; Heyde, M.; Shaikhutdinov, S.; Freund, H.-J.; Włodarczyk, R.; Sierka, M.; Sauer, J. *Phys. Rev. Lett.* **2010**, *105*, 146104.
(15) Heyde, M.; Shaikhutdinov, S.; Freund, H.-J. *Chem. Phys. Lett.* **2012**, *550*, 1−7.
(16) Huang, P. Y.; Kurasch, S.; Srivastava, A.; Skakalova, V.; Kotakoski, J.; Krasheninnikov, A. V.; Hovden, R.; Mao, Q.; Meyer, J. C.; Smet, J.; Muller, D. A.; Kaiser, U. *Nano Lett.* **2012**, *12*, 1081−1086.
(17) Oganov, A. R.; Glass, C. W. *J. Chem. Phys.* **2006**, *124*, 244704.
(18) Oganov, A. R.; Lyakhov, A. O.; Valle, M. *Acc. Chem. Res.* **2011**, *44*, 227−237.
(19) Lyakhov, A. O.; Oganov, A. R.; Stokes, H. T.; Zhu, Q. *Comput. Phys. Commun.* **2013**, *184*, 1172−1182.
(20) Mannix, A. J.; Zhou, X.-F.; Kiraly, B.; Wood, J. D.; Alducin, D.; Myers, B. D.; Liu, X.; Fisher, B. L.; Santiago, U.; Guest, J. R.; Yacaman, M. J.; Ponce, A.; Oganov, A. R.; Hersam, M. C.; Guisinger, N. P. *Science* **2015**, *350*, 1513−1516.
(21) Niu, H.; Oganov, A. R.; Chen, X.-Q.; Li, D. *Sci. Rep.* **2015**, *5*, 18347.
(22) Dong, X.; Li, Y.-L.; Oganov, A. R.; Li, K.; Zheng, H.; Mao, H.-k. arXiv:1603.02880 2016.
(23) Wang, Y.; Lv, J.; Zhu, L.; Ma, Y. *Phys. Rev. B: Condens. Matter Mater. Phys.* **2010**, *82*, 094116.
(24) Perdew, J. P.; Burke, K.; Ernzerhof, M. *Phys. Rev. Lett.* **1996**, *77*, 3865−3868.
(25) Blöchl, P. E. *Phys. Rev. B: Condens. Matter Mater. Phys.* **1994**, *50*, 17953−17979.
(26) Kresse, G.; Joubert, D. *Phys. Rev. B: Condens. Matter Mater. Phys.* **1999**, *59*, 1758−1775.
(27) Kresse, G.; Furthmüller, J. *Phys. Rev. B: Condens. Matter Mater. Phys.* **1996**, *54*, 11169−11186.
(28) Kresse, G.; Furthmüller, J. *Comput. Mater. Sci.* **1996**, *6*, 15−50.
(29) Blöchl, P. E.; Jepsen, O.; Andersen, O. K. *Phys. Rev. B: Condens. Matter Mater. Phys.* **1994**, *49*, 16223−16233.
(30) Perdew, J. P.; Zunger, A. *Phys. Rev. B: Condens. Matter Mater. Phys.* **1981**, *23*, 5048−5079.
(31) Heyd, J.; Scuseria, G. E.; Ernzerhof, M. *J. Chem. Phys.* **2003**, *118*, 8207−8215.
(32) Togo, A.; Oba, F.; Tanaka, I. *Phys. Rev. B: Condens. Matter Mater. Phys.* **2008**, *78*, 134106.
(33) Pauling, L. *The Nature of the Chemical Bond*, 3rd ed.; Cornell University Press: Ithaca, NY, 1960.
(34) Xu, W.; Zhang, G.; Li, B. *J. Chem. Phys.* **2015**, *143*, 154703.
(35) Smyth, J. R.; Swope, R. J.; Pawley, A. R. *Am. Mineral.* **1995**, *80*, 454−456.
(36) Glsplnrr, T. *Am. Mineral.* **1990**, *75*, 739−747.
(37) Dera, P.; Prewitt, C. T.; Boctor, N. Z.; Hemley, R. J. *Am. Mineral.* **2002**, *87*, 1018−1023.
(38) Weiss, A.; Weiss, A. *Z. Anorg. Allg. Chem.* **1954**, *276*, 95−112.
(39) Deer, W. A.; Howie, R. A.; Zussman, J. *An Introduction to the Rock-forming Minerals*, 2nd ed.; Longman Scientific and Technical: Essex, 1992; pp 1−696.
(40) Zhang, S.; Zhou, J.; Wang, Q.; Chen, X.; Kawazoe, Y.; Jena, P. *Proc. Natl. Acad. Sci. U. S. A.* **2015**, *112*, 2372−2377.
(41) Franklin, A. D. *Science* **2015**, *349*, aab2750.
(42) Bonaccorso, F.; Colombo, L.; Yu, G.; Stoller, M.; Tozzini, V.; Ferrari, A. C.; Ruoff, R. S.; Pellegrini, V. *Science* **2015**, *347*, 1246501.
(43) Landau, L. D.; Lifshitz, E. M. *Theory of Elasticity*; Pergamon: Oxford, 1995.
(44) Lakes, R. *Science* **1987**, *235*, 1038−1040.
(45) Jiang, J.-W.; Chang, T.; Guo, X.; Park, H. S. *Nano Lett.* **2016**, *16*, 5286−5290.
(46) Jiang, J.-W.; Park, H. S. *Nano Lett.* **2016**, *16*, 2657−2662.
(47) Jiang, J.-W.; Park, H. S. *Nat. Commun.* **2014**, *5*, 4727.
(48) Du, Y.; Maassen, J.; Wu, W.; Luo, Z.; Xu, X.; Ye, P. D. *Nano Lett.* **2016**, *16*, 6701−6708.
(49) Jiang, J.-W.; Kim, S. Y.; Park, H. S. *Appl. Phys. Rev.* **2016**, *3*, 041101.
(50) Özçelik, V. O.; Cahangirov, S.; Ciraci, S. *Phys. Rev. Lett.* **2014**, *112*, 246803.
(51) Wang, Y.; Li, F.; Li, Y.; Chen, Z. *Nat. Commun.* **2016**, *7*, 11488.
(52) Baughman, R. H.; Shacklette, J. M.; Zakhidov, A. A.; Stafström, S. *Nature* **1998**, *392*, 362−365.
(53) Grima, J. N.; Evans, K. E. *J. Mater. Sci.* **2006**, *41*, 3193−3196.
(54) Liu, Q. *Literature review: materials with negative Poisson's ratios and potential applications to aerospace and defence*; DSTO, Defence Science and Technology Organisation: 2006.
(55) Wei, X.; Fragneaud, B.; Marianetti, C. A.; Kysar, J. W. *Phys. Rev. B: Condens. Matter Mater. Phys.* **2009**, *80*, 205407.
(56) Sánchez-Portal, D.; Artacho, E.; Soler, J. M.; Rubio, A.; Ordejón, P. *Phys. Rev. B: Condens. Matter Mater. Phys.* **1999**, *59*, 12678−12688.
(57) Wei, Q.; Peng, X. *Appl. Phys. Lett.* **2014**, *104*, 251915.
(58) Qiao, J.; Kong, X.; Hu, Z.-X.; Yang, F.; Ji, W. *Nat. Commun.* **2014**, *5*, 4475.
(59) Keskar, N. R.; Chelikowsky, J. R. *Nature* **1992**, *358*, 222−224.
(60) Wu, X.; Varshney, V.; Lee, J.; Zhang, T.; Wohlwend, J. L.; Roy, A. K.; Luo, T. *Nano Lett.* **2016**, *16*, 3925−3935.
(61) Wu, X.; Varshney, V.; Lee, J.; Pang, Y.; Roy, A. K.; Luo, T. arXiv:1607.06542 2016.
(62) Zubov, V.; Firsova, M. *Soviet. Phys. Cryst.* **1962**, *7*, 374−376.
(63) Ohno, I. *J. Phys. Earth* **1995**, *43*, 157−169.
(64) Kimizuka, H.; Ogata, S.; Li, J.; Shibutani, Y. *Phys. Rev. B: Condens. Matter Mater. Phys.* **2007**, *75*, 054109.
(65) Andrew, R. C.; Mapasha, R. E.; Ukpong, A. M.; Chetty, N. *Phys. Rev. B: Condens. Matter Mater. Phys.* **2012**, *85*, 125428.

DOI: 10.1021/acs.nanolett.6b03921
Nano Lett. 2017, 17, 772−777